



Original Articles

Rational design and development of a peptide inhibitor for the PD-1/PD-L1 interaction



Rebecca J. Boohaker^{a, b, **}, Vijaya Sambandam^a, Isaac Segura^c, James Miller^d,
Mark Suto^a, Bo Xu^{a, b, e, *}

^a Southern Research Institute, Drug Discovery Division, Birmingham, AL, 35205, USA

^b University of Alabama at Birmingham Comprehensive Cancer Center, Department of Cell, Developmental and Integrative Biology, Birmingham, AL, 35294, USA

^c Spring Hill College, Department of Chemistry, Mobile, AL, 36608, USA

^d Wake Forest University, Department of Chemistry, Winston-Salem, NC, 27109, USA

^e Key Laboratory of Breast Cancer Prevention and Therapy, Ministry of Education, Tianjin's Clinical Research Center for Cancer, Tianjin Medical University Cancer Institute and Hospital, National Clinical Research Center for Cancer, Tianjin, China

ARTICLE INFO

Article history:

Received 10 February 2018

Received in revised form

13 April 2018

Accepted 22 April 2018

Keywords:

PD-1

Peptide therapy

Immune checkpoints

CD8 T-cells

ABSTRACT

We report here the rational design and validation of a peptide inhibitor to the PD-1/PD-L1 interaction as an attempt to develop a viable alternative to current inhibitory antibodies. We demonstrated, by biolayer interferometry and *in silico* docking simulations, that a PD-L1 peptide mimetic (PL120131) can interfere with the PD-1/PD-L1 interaction by binding to PD-1. We show that PL120131 is capable of inhibiting PD-1 mediated apoptotic signaling pathway and rescuing Jurkat cells and primary lymphocytes from apoptosis. Additionally, we show that PL120131 treatment allows for CTL anti-tumor activity. Furthermore, PL120131 can maintain co-culture survivability and activity of T Cells in a 3D co-culture model better than the anti-PD-1 blocking antibody. Together, the characterization of this PD-1/PD-L1 inhibiting peptide provides insight regarding the ability to inhibit PD-L1 binding while maintaining CTL viability and activity that can further the development of alternatives to antibody based immunotherapies.

© 2018 Published by Elsevier B.V.

1. Introduction

Programmed Cell Death Protein-1 (PD-1, or CD279) is a member of the B7-CD28 superfamily, which is important in the regulation of immune system components, specifically T-cells and natural killer (NK) cells [1–3]. The PD-1 pathway is critical in normal immune homeostasis as it functions to promote tolerance and minimize chronic inflammation [4]. This surface receptor and its predominant ligand, programmed death-ligand-1 (PD-L1, or CD274), have become prime therapeutic targets for overcoming tumor-induced immune evasion [5]. While the PD-1/PD-L1 mechanism is typically a necessary regulatory pathway for maintaining immune homeostasis, high PD-L1 expression on tumor cells has been linked

to poor prognosis and is an indicator of the immune evasion survival mechanism [6,7].

In recent years, there has been a focus on the development of T-cell-mediated immunotherapy against cancer. Immunotherapy has progressed from FDA approval of IL-2 infusions which promotes T-cell proliferation in the treatment of metastatic renal carcinoma in 1992 [8] to the development of chimeric antigen receptor therapy (CAR-T) to recognize tumor neo-antigens and the use of checkpoint inhibiting antibodies. The common thread of these methods is the goal of retaining active tumor infiltrating lymphocytes (TILs). Each of these therapeutic avenues has advanced the field of immunology while also encountering with certain obstacles.

Based on an understanding of the immune system's self-regulatory mechanisms, certain TIL surface receptors have been targeted for the development of inhibitory antibodies. Of note, the predominant candidate receptors are CTLA-4, LAG-3, BTLA, TIGIT, TIM-3 and PD-1 that are expressed in an exhausted T-cell phenotype [9–11]. Additionally, the converse strategy of targeting PD-L1 on tumors and other regulatory components of the local immune environment has also been explored. Antibodies raised to PD-1 (e.g.

* Corresponding author. Department of Oncology, Southern Research Institute, 2000 9th Ave South, Birmingham, AL, 35205, USA.

** Corresponding author. Department of Oncology, Southern Research Institute, 2000 9th Ave South, Birmingham, AL, 35205, USA.

E-mail addresses: rboohaker@southernresearch.org (R.J. Boohaker), bxu@southernresearch.org (B. Xu).

Pembrolizumab and Nivolumab) or PD-L1 (Atezolizumab) have been granted accelerated FDA approval and are currently being used in clinic for the treatment of certain malignancies, specifically melanomas and non-small cell lung carcinomas (NSCLCs) [12–14]. Given the success and improved response rates in these instances, these therapies are being used in increasingly varied cancer types, particularly those resistant to classical chemotherapies and expressing high levels of PD-L1. These adverse effects, while often reversible, can result in permanent damage to vital organs if left unchecked [15]. A second-generation therapy that builds on the proof-of-principle of the antibody therapy can expand the success of targeting this specific immune-checkpoint while minimizing or eliminating the unintended triggering of auto-immune symptoms.

A solved crystal structure of the extracellular domains of PD-1 and PD-L1 [16] provides insight into the specific structural interactions of the two proteins, with specific interest on the PD-1 binding domain. Analysis of the two structures indicates that a competitive inhibitor could be designed to fit into the PD-L1 binding site, effectively displacing PD-L1 and any other redundant or secondary ligands such as PD-L2. These results are in stark contrast to recent attempts of designing inhibitors for this interaction via disruption of PD-L1 homo-dimerization [17], which would be a less direct means of inhibition to a ligand that may or may not be expressed on the target tumor cell. To that end, we have designed a peptide mimetic of PD-L1 to act as a competitive inhibitor of the PD-1/PD-L1 interaction that binds to the singular PD-L1 binding domain of PD-1. The experiments outlined below systematically demonstrate the ability of the 12-mer to bind PD-1 and displace PD-L1 in cell-free binding experiments. We show that the 12-mer can reverse the apoptotic signal in Jurkat and isolated murine primary lymphocytes exposed to soluble PD-L1. These primary lymphocytes, treated with our peptide inhibitor, are able to maintain viability and activity in the presence of soluble PD-L1 and in co-culture with PD-L1 expressing tumor cell lines.

Our data addresses the design, selectivity and efficacy of a peptide inhibitor to the PD-1/PD-L1 immune checkpoint as a viable alternative to current inhibitory antibodies.

2. Results

2.1. Design of inhibiting peptides for PD-1/PD-L1

Examination of the solved X-ray crystal structure [16] of the extracellular, soluble fractions of PD-1 and PD-L1 indicate a series of interacting residues on both proteins. PD-1 interacting residues are contained within the primary sequence spanning the methionine at position 64 to the lysine at position 78 (PD6478). The interacting residues on PD-L1 comprise a contiguous span of amino acids from glycine at position 120 to asparagine at 131 (PL120131). Not coincidentally, our PL120131 peptide also contains two “anchor” residues as determined by *in silico* modeling [18]. A protein blast of these sequences indicates that the sequences are highly conserved across species (Fig. 1A).

In Silico binding studies were done using CABS-doc and MOE to determine the most probable orientation and theoretical binding energies for each peptide sequence. Fig. 1B models the binding of the PD-L1 derived peptide to the soluble fraction of PD-1. The secondary structure of PD-1 is such that a singular natural binding pocket is also the site for PD-L1 interaction as determined by the solved crystal structure [16]. To determine if PL120131 would readily associate with this natural binding site, the CABS-dock simulation was conducted as a blind docking simulation, with no bias to any particular region of PD-1. The top three docking orientations are shown and all associate exclusively with the shallow binding pocket of PD-1.

The theoretical binding energy was determined by MOE, and the resulting space filling model shows the shallow binding groove in PD-1 occupied by the PL120131 peptide in purple (Fig. 1C). The resultant binding energy was determined to be -10.28 kJ. This is the calculated energy for the top conformation of 30 attempts. Fig. 1D gives a detailed interaction map of the peptide with the receptor residues. In orange are the residues within the binding pocket that contribute to the peptide association.

2.2. Synthetic peptide blocking of PD-L1 binding in a cell-free system

In order to validate the results of the *in silico* docking simulations, cell-free, biolayer interferometry studies were conducted using synthetic peptide and purified recombinant protein. Biolayer interferometry allows for a calculation of binding coefficients by measuring the difference in interference signal with, and without, bound ligand. Validation of the *in silico* docking simulation was done by determining the binding coefficient of recombinant PD-1 with recombinant PD-L1. For peptide binding studies, His-PD-1 was immobilized on an anti-His biosensor at a fixed concentration. Binding of PL120131 or PD6478 to immobilized PD-1 was then measured in serial dilution. The resulting interferograms (Fig. 2A and B) show that PL120131 has a higher affinity of binding to PD-1 than PD6478, validating the *in silico* modeling which indicated that PD6478 is a poor binder to PD-1.

We then established the binding constant for the uninhibited interaction by running a dilution series of the extracellular domain of PD-L1 against a fixed concentration of HIS-PD-1 and found that the calculated K_D of PD-1 and PD-L1 was 3.05×10^{-7} M (Fig. 2C). Using this measure as an indicator of no inhibition, we conducted a competition assay to determine if the peptides could competitively inhibit PD-L1 binding to PD-1. To do this, a similar BLI experiment was run holding the concentrations of the two recombinant proteins constant while increasing the concentration of PL120131 and PD6478 respectively. Fig. 2D shows the association rate K_D of PD-L1 to PD-1. PL120131 was able to reduce association of PD-L1 in a dose dependent manner. PD6478 concentrations did not affect PD-L1 association rates. This correlates with the *in silico* data suggesting that PL120131 acts as a competitive inhibitor of PD-L1 binding by associating with the binding groove in PD-1.

2.3. Inhibition of PD-1 apoptotic signaling pathway and rescue of Jurkat cells and primary lymphocytes from apoptosis

We assessed two parameters to test whether PL120131 was effective in disrupting the PD-1 signaling pathway. The first was via a luciferase reporter PD-1/PD-L1 blockade assay in which T-cell Receptor (TCR) mediated activation of a NFAT-RE results in luciferase production when the checkpoint is blocked. The effector Jurkat cells containing the NFAT-RE-Luciferase element and the PD-L1 expressing CHO cells were co-cultured with either the monoclonal J116 anti-PD-1 antibody, the PD6478, or PL120131 in an overnight treatment. The measure of luminescence across doses indicates that PL120131 has a lower ED_{50} at 0.296 than the anti-PD-1 antibody ($ED_{50} = 0.874$). PD6478 did not show an effective blockade across doses (Fig. 3). This confirms that the peptide PL120131 is indeed acting as a checkpoint inhibitor.

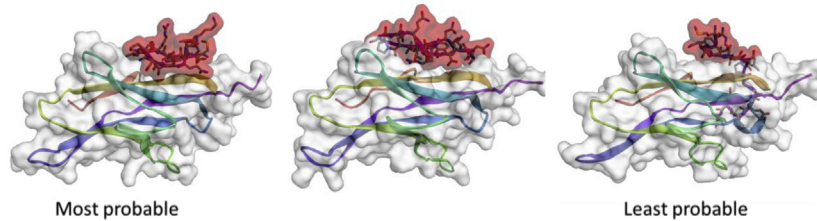
Since PD-1 is a sensor receptor in a death pathway, and given that our intent is to target the binding site for direct inhibition, we had to determine that peptide binding was not triggering the activation of the death pathway, as PD-L1 would. A major consideration for an immune checkpoint inhibitor is whether or not the inhibition can reverse or block the signaling cascade initiated by the engagement of the receptor. In this case, we show that PD-1

A

PD-1 Derived Inhibiting Peptide: PD6478

Homo sapiens	MLNWNRLSPSNQTEK
Mus musculus	V LNWY R MSPSNQTDK
Microtus ochrogaster	K LNWYRLSPSNQTDK
Bos taurus	-LNWY R KSPSNQMDK
Glossina fuscipes fuscipes (Tsetse Fly)	MLNWNRL V P-----

Model	Cluster Density	Average RMSD	Max RMSD
Orientation 1	28.1344	6.54003	18.178
Orientation 2	10.3761	8.28825	20.3616
Orientation 3	5.11414	13.6875	28.0393

**B**

PD-L1 Derived Inhibiting Peptide: PL120131

Homo sapiens	GADYKRITVKVN
Mus musculus	GADYKRIT L KVN
Oryctolagus cuniculus	GADYKRIT L KVN
Bos taurus	GADYKRIT L KVN
Danio rerio	--DYK Q IT L NV--

Model	Cluster Density	Average RMSD	Max RMSD
Orientation 1	19.0296	7.67226	28.0924
Orientation 2	13.8344	11.4208	25.0542
Orientation 3	6.26233	11.8167	34.6806

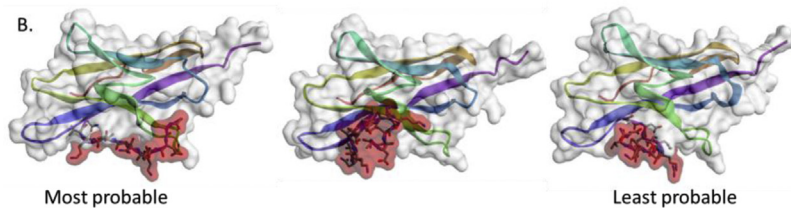
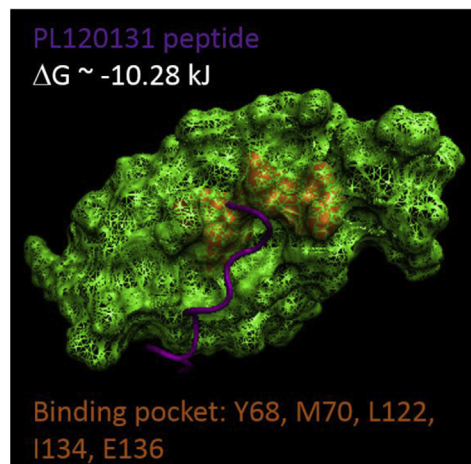
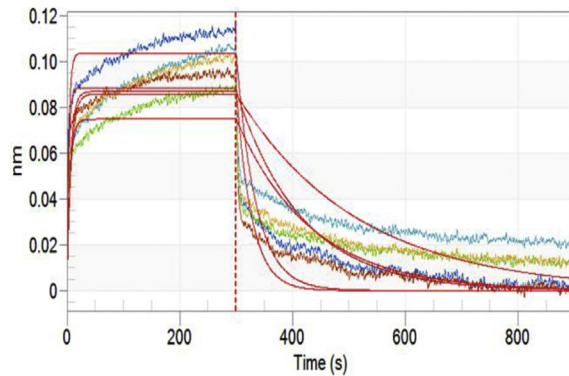
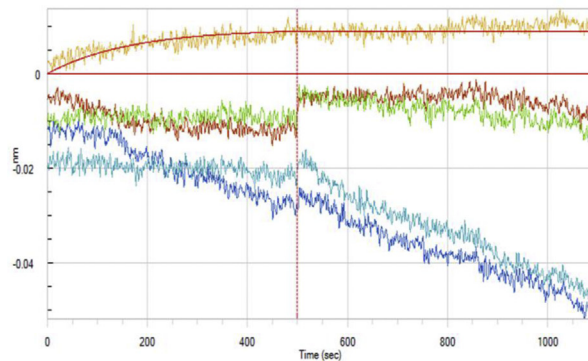
**C**

Fig. 1. Rational Peptide Design and *in silico* docking simulations. Peptide sequences derived from PD-1 (A) and PD-L1 (B) determined by contact residues from the crystal structure were verified for cross-species homology. The peptides are shown in their “best-fit” orientations. The most probable fit of the PL120131 (purple) to the PD-1 (green) was run in a docking simulation to calculate ΔG the resulting PDB coordinates are displayed in (C). The orange region highlights the theoretical interaction sites on PD-1. (For interpretation of the references to colour in this figure legend, the reader is referred to the Web version of this article.)

A

[PL120131]	KD (M)	KD Error
2 μ M	1.31E-05	1.54E-06
0.67 μ M	5.29E-06	6.18E-07
0.22 μ M	4.58E-07	5.91E-08
0.074 μ M	1.93E-07	2.70E-08
0.024 μ M	8.39E-08	1.08E-08

B

[PD6478]	KD (M)	KD Error
120 μ M	5.31E+22	2.87E+54
40 μ M	6.68E-12	2.62E+18
13.2 μ M	2.59E+14	1.04E+39
4.44 μ M	1.06E+21	<1.0E-12
1.48 μ M	<1.0E-12	7.26E-09

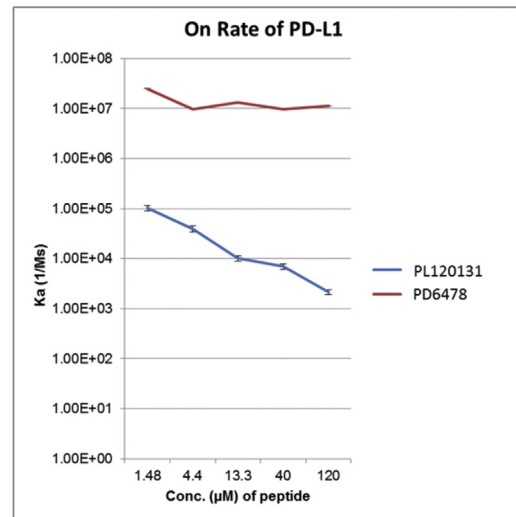
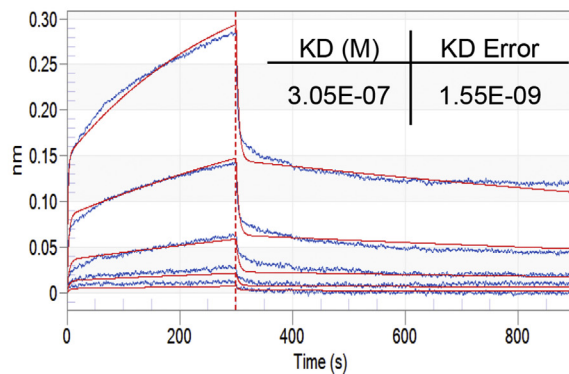
C

Fig. 2. Bi-layer Interferometry Indicates PL120131 Inhibits PD-L1 binding in a Dose-Dependent Manner. Bi-layer interferometry (BLI) quantification of the binding of PL120131 (A) or PD6478 (B) to recombinant PD-1 shows that PL120131 has affinity for PD-1. The baseline affinity of recombinant PD-L1 for PD-1 is shown in (C). A competition assay to measure the association of PD-1 to PD-L1 in the presence of increasing concentrations of either PL120131 or PD6478 was also measured by BLI.

mediated apoptotic cell death in Jurkat cells can be initiated solely by exposure to soluble PD-L1. This occurs in a dose dependent manner and mimics the death induced by staurosporine treatment, a positive apoptotic agent (Fig. 4A–C). From this dose response an IC_{50} for PD-L1 was determined to be 12 μ M, and incubation with PL120131 in increasing concentrations resulted in a 25% reduction

in early and late apoptotic signals as measured by Annexin V and Caspase 3/7 staining respectively.

This was repeated with mouse primary lymphocytes with a focus on the viability of the lymphocyte population post treatment with PL120131 showing a significant rescue of cell viability. Importantly, treatment with PL120131 alone did not reduce T-cell

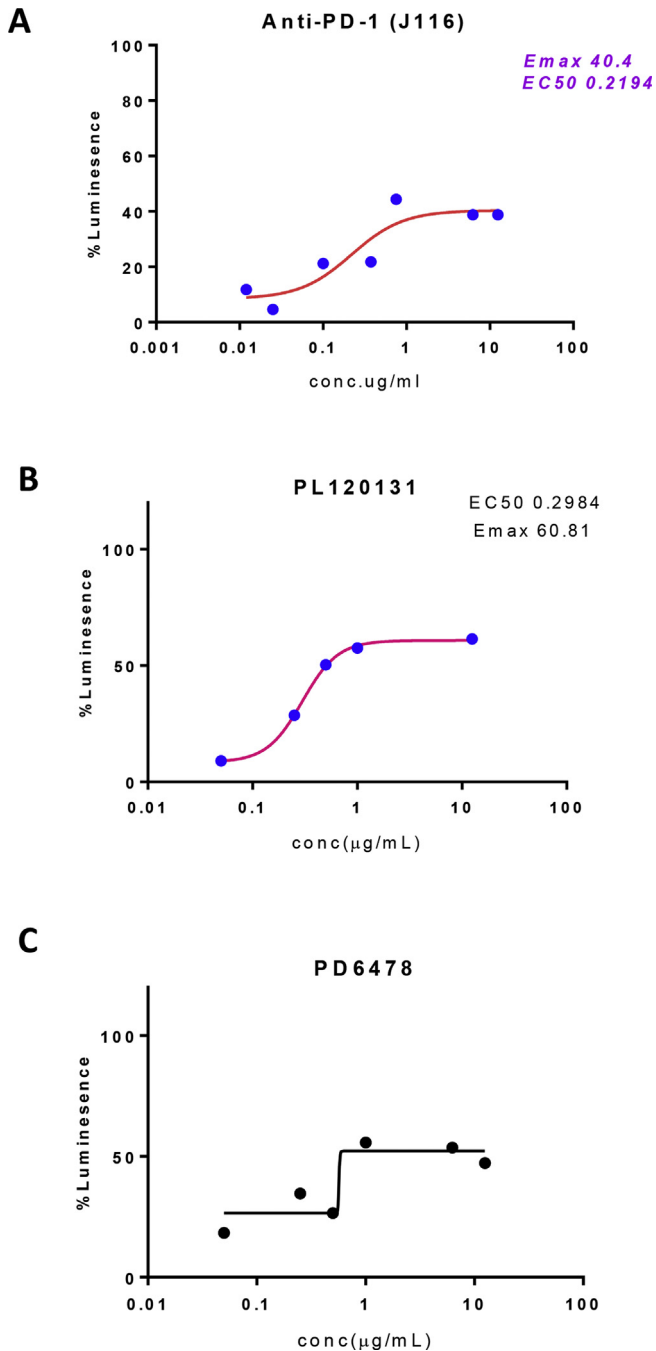


Fig. 3. PL120131 Blocks the PD-1/PD-L1 interaction in co-culture. A PD-1/PD-L1 checkpoint luciferase reporter assay (RE-NFAT) was used to examine the effects on signaling pathways. The dose response curves for the Anti-PD-1 blocking antibody (A), PL120131 (B), and PD6478 (C) are shown. The EC_{50} for the antibody and PL120131 were able to be calculated, but not the PD6478. Luminescence is normalized to the measure of untreated Jurkat cells.

viability (Fig. 4D). In order to test this inhibition against normal, non-immortalized cells, we co-cultured human peripheral blood mononuclear cells (PBMCs) with MDA-MB-231 cells for 24 h. The cells were then stained for CD3, CD45, and CD8. The CD3/CD45/CD8 cells were quantified by flow cytometry. There is an increase in these cells with both the anti-PD-1 (J116) and the PL120131 peptide, but not PD6478 (Fig. 4E). This taken with the BLI data indicates that PL120131 is 1) binding to PD-1 2) in a competitive manner, and 3) without engaging the PD-1 apoptotic signaling pathway.

2.4. Co-culture survivability and activity of T cells are maintained upon treatment with PL120131

Exhaustion of a previously active CD8 T-cell population is the result of prolonged exposure to an antigen stimulus in an inflammatory environment [19]. The ability for CD8 T-cells to maintain their activity in such an environment was tested by co-culturing primary lymphocytes in the presence of the PD-L1 expressing cell line 4T1 is necessary for anti-tumor activity. 4T1 cells were cultured with primary lymphocytes in a 1:2 ratio (Fig. 5A). It was observed that treatment with PL120131 at an EC_{50} of $11.6\mu\text{M}$ was sufficient to rescue primary t-cells from apoptosis. Analysis of the 4T1 cells indicated an increase in cell death. To determine if this 4T1 cell death is due to cytotoxic T-cell activity, the activation chemokine, granzyme B, was measured by flow cytometry (Fig. 5B). The Granzyme B production of primary CD8⁺ T-cells was assessed after 24- hour co-culture with PD-L1 expressing 4T1 cells. 6 h prior to harvesting, GolgiStop was added to the culture to halt the secretion of Granzyme B. Flow cytometry analysis of CD3⁺/CD8⁺ T-cells indicates that when treated with PL120131, there is a significant increase in Granzyme B production relative to mock treated, PD6478, and even the inhibitory anti-PD-1 antibody (Fig. 5C). This increase in Granzyme B production is dose dependent (Fig. 5D).

Additionally, we examined the secretion of cytokines from cells in co-culture. Specifically, we focused on IL-10, IL-12p70, and IFN γ (Fig. 6A and C) as measures of CD8 T-cell activation. We also looked at the production of CCL4 (Fig. 6D), a recruitment cytokine. IFN γ levels were found to increase in a dose dependent manner, which is indicative of activated T-cells, thereby verifying the Granzyme B production (Fig. 6A). The inhibiting cytokines IL-10 and IL-12 (p70) showed a dose dependent decrease in response to PL120131 treatment (Fig. 6B and C). This indicates that the peptide treatment is overriding the checkpoint signal presented by the 4T1 cells.

2.5. PL120131 treated T-cells infiltrate the tumor microenvironment in 3D culture

To evaluate the efficacy of PL120131 as a checkpoint inhibitor in a 3D environment, artificial MDA-MB-231 tumors were seeded in a human fibronectin extra-cellular matrix (ECM) in the central chamber of a microfluidics chip. Cell Tracker labeled Jurkat cells with and without checkpoint inhibitors were injected into a vascular channel at a physiological flow rate of $0.2\mu\text{L}/\text{min}$. The SynVivo system is intended to approximate an *in vivo* environment [20–22], and is particularly suitable for measuring trafficking and migration of our target cells into a “solid tumor” environment. Cells were imaged over the course of an hour to ensure that they infiltrated into the central chamber (Supplemental Fig. 1). The now mixed population of cells in the central chamber was flushed, fixed, and stained with Annexin V. Apoptotic analysis by Annexin V staining of the infiltrating Jurkat vs MDA-MB-231 cells shows tumor line cell death in both J116 and PL120131 treated cells; however, the PL120131 treated Jurkat cells are markedly more effective in killing than the J116 treated counterparts (Fig. 7).

Time-lapse imaging of the primed Jurkat cells show that they traffic into to the tumor environment and engage with the tumor cell line within the first hour of exposure (Supplemental Video 1). This is critical because it indicates that despite expression of PD-L1 on the MDA-MB-231 cells, there is not an ECM barrier preventing Jurkat infiltration.

Supplementary video related to this article can be found at <https://doi.org/10.1016/j.canlet.2018.04.031>.

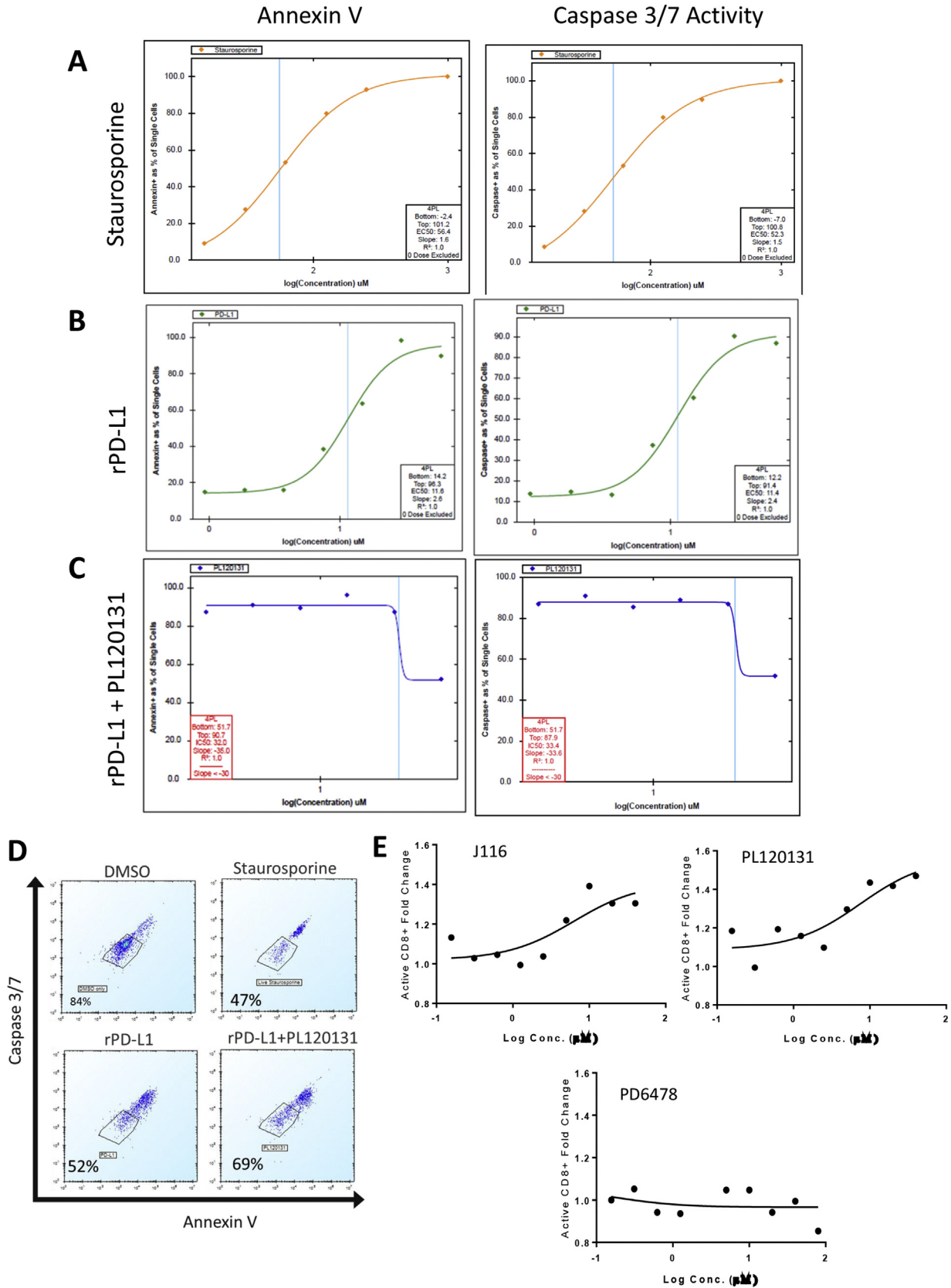


Fig. 4. PL120131 inhibition is sufficient to rescue viability of Primary lymphocytes. Annexin V and Caspase3/7 levels in primary mouse lymphocytes quantify apoptotic cell death in the presence of recombinant PD-L1. A dose response of staurosporine, recombinant PD-L1, or PL120131 was tested for the extent of apoptotic death (A–C). A dot plot representation (D) of the EC₅₀ treatments for each data point are gated on the viable (Annexin V (–), Caspase 3/7 (–)) population. Human PBMCs treated with anti-PD1 or PL120131 allow for the proliferation of CD8⁺ T-cells in a dose dependent manner (E). PD6478 treated PBMCs remain non-proliferative regardless of concentration.

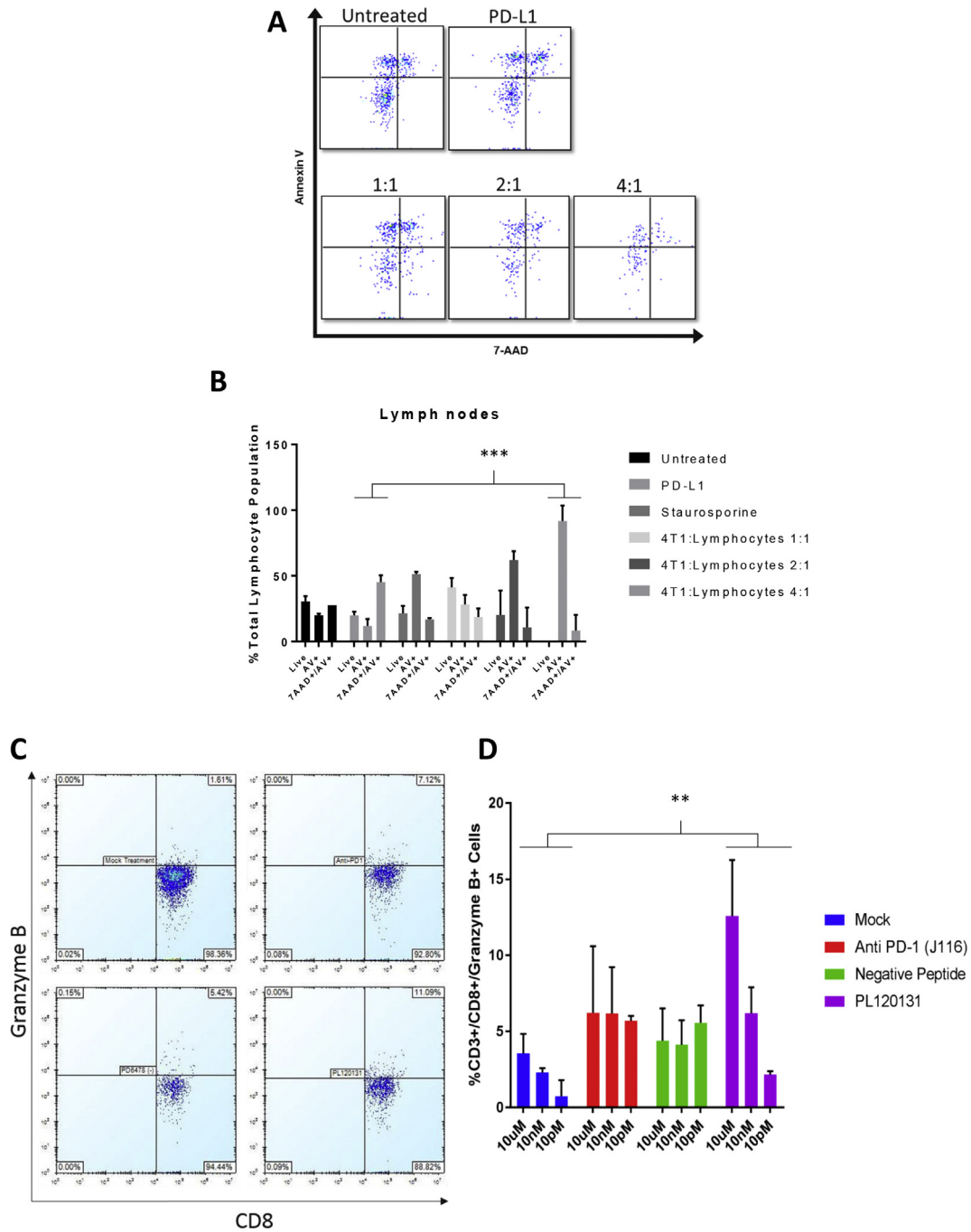


Fig. 5. PL120131 treatment maintains cytotoxic activity of T-cells in co-culture. Primary mouse lymphocytes in co-culture with increasing amounts of 4T1 murine breast cancer cells (A) show that the number of PD-L1-expressing 4T1 cells affects the viability of primary lymphocytes. Primary lymphocytes isolated from C57BL6 mice in 1:1 co-culture with 4T1 cells are gated on CD3⁺ cells. Quantification of the viability is seen in (B). Dot plots the 10 µM treatments of CD3⁺ cells are plotted as CD8 vs Granzyme B (C). Dose responses were plotted and show a dose effect with PL120131 (D). Measurements were taken 24 h after treatment. A 2-way Anova of the row populations shows the significant changes in viability (B) and Cytokine production (D) when cultured with PD-L1 expressing 4T1 cells. P < 0.05 = *, P < 0.005 = **, P < 0.0001 = ***. For Granzyme B, F = 24.38 and P = 0.0017. Each experiment was done in triplicate. Within each experiment, each condition was measured in duplicate.

3. Discussion

The results outlined above systematically demonstrate the ability of the 12-mer to bind PD-1 and displace PD-L1 in cell-free binding experiments. We show that the 12-mer can reverse the apoptotic signal in Jurkat and isolated murine primary lymphocytes exposed to soluble PD-L1. These primary lymphocytes, treated with our peptide inhibitor, are able to maintain viability and activity in

the presence of soluble, recombinant PD-L1 and in co-culture with PD-L1 expressing tumor cell lines.

The blocking of the dominant binding site of PD-1 with a peptide mimic of its native ligand provide insight into the ability to block the interaction of PD-L1, and likely PD-L2, without engaging the PD-1 receptor pathway. This is critical because, to date, blocking antibodies, while effective, only provide a steric barrier to PD-1 engagement and do not act as a direct inhibitor to the interaction.

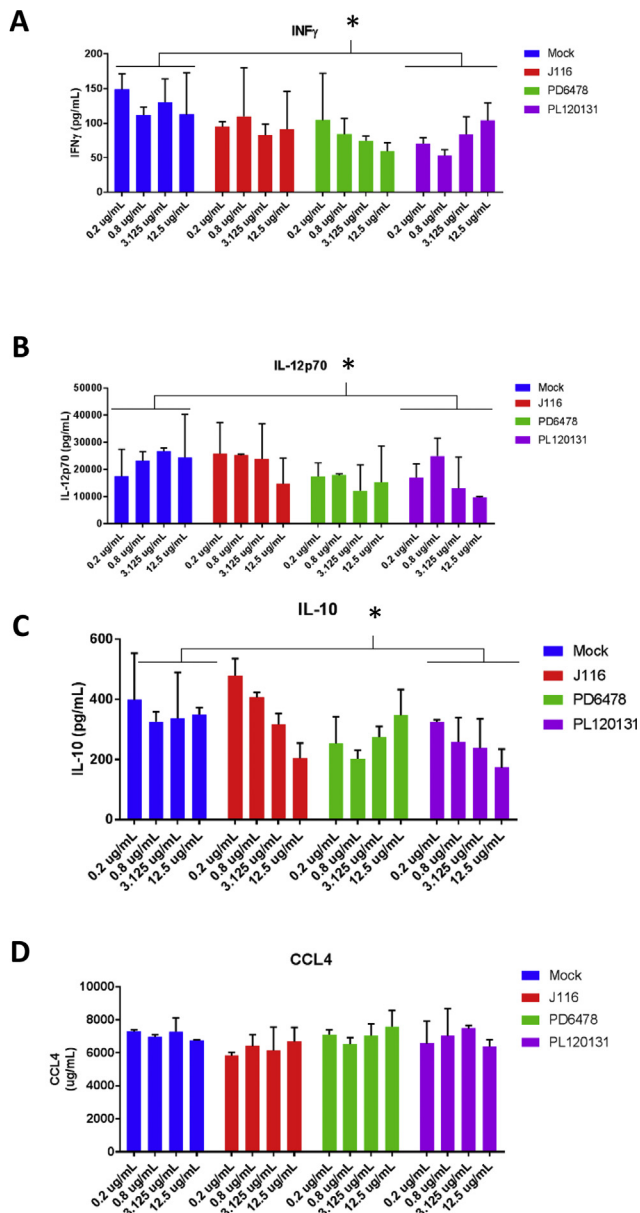


Fig. 6. Key regulatory cytokines are affected when treated with PL120131. A measure of cytokine release by cells in co-culture was done by cytokine capture beads and read by flow cytometry (A: IFN γ , B: IL-12p70, C: IL-10, and D: CCL4). Mouse primary lymphocytes were dosed with DMSO, PD-1 blocking antibody, PD6478, or PL120131 prior to co-culture. Measurements were taken 24 h after treatment. A 2-way Anova of the row populations shows the significant changes in Cytokine production when cultured with PD-L1 expressing 4T1 cells. $P < 0.05 = *$, $P < 0.005 = **$, $P < 0.0001 = ***$. For IFN γ , $F = 10.75$ and $P = 0.0112$. For IL-12p70, $F = 7.91$ and $P = 0.0315$. For IL-10, $F = 5.063$ and $P = 0.0256$. No significance in CCL4 was found across treatments. Each experiment was done in triplicate with duplicate measures per condition per experiment.

Our data collectively shows that in the presence of a specific inhibitory signal, either as recombinant protein or expressed on the surface of tumor cells, we can maintain T-cell populations, both in viability and activity.

Peptide mimics, as a class of therapeutics, have lower half-life and significantly smaller size, are able to penetrate into solid tumors and tissues better than antibodies, and they are ideal as inhibitors for the PD1/PD-L1 interaction. However, efforts toward this direction has been limited. A recent report using computational de novo peptide design have yielded several PD-1 binding peptides,

however no relevant biological activities were tested [18]. It is critical to state that the design and development of our inhibiting peptide involved not only the characterization of binding in a cell-free system, but also evaluation of the effects of PL120131 on the biochemical pathways responsible for the desired T-cell functionality. This is particularly important when evaluating these, or any, inhibitors in the context of a tumor microenvironment. One significant hurdle in immune-oncology is that a substantial number of non-T-cell inflamed solid tumors are impervious to invasive CTLs [23]. In the increasingly complex *in vitro* systems presented, we have attempted to recreate such an environment to provide a comprehensive assessment of the efficacy PL120131 checkpoint inhibition. Further testing, both using *ex vivo* expansion of CTLs and *in vivo* dosing with PL120131, or small-peptide derivatives, will provide useful information regarding efficacy against solid tumors and the durability of the response with regards to the ability to generate and maintain immunological Memory.

Checkpoint inhibitors provide a significant paradigm shift in the way that cancer is treated. Rather than targeting an ever changing, heterogeneous tumor, harnessing the inherent killing ability of the immune system has been shown to be more effective in inducing tumor cell death. The current, and emerging use of checkpoint inhibiting antibodies as frontline standard-of-care therapies in numerous tumor types provides clinical evidence that checkpoint blockades are a viable therapeutic strategy. The development of specific, competitive inhibitors to these checkpoint proteins will expand on the existing therapies. Here, we provide evidence of the ability to target the specific binding site on PD-1 without triggering the PD-1 cell death cascade. This is proof-of-principle that small molecules or truncated peptides and peptide mimetics can be designed toward the PD-1 binding domain.

4. Methods

4.1. Cell lines and primary cell culture

Jurkat (clone E6-1 ATCC TIB-152), MDA-MB-231 (ATCC HTB-26), and 4T1 (ATCC CRL-2539) cells were obtained from ATCC. MDA-MB-231 cells were cultured in DMEM media supplemented with 1% Penicillin/Streptomycin and 10% Fetal Bovine Serum (FBS). Jurkat cells were cultured in RPMI 1640 media with 1% Penicillin/Streptomycin and 10% Fetal Bovine Serum. 4T1 cells were cultured in RPMI 1640 supplemented with 10% FBS, 1% Pen/Strep, 4.5 g/L glucose, 2 mM L-glutamine, 10 mM HEPES, 1 mM sodium pyruvate, and 1.5 g/L sodium bicarbonate.

Mouse primary lymphocytes were obtained from normal C57BL/6 males at 3 months of age. The lymph nodes of 6 mice were pooled to obtain a sufficient number of cells for each experiment. Primary lymph nodes were dissected out and homogenized through a 0.2 μ m nylon mesh filter into RPMI 1640 complete media. The cells were spun down at 800 g and resuspended for viability count. Human PBMCs were obtained from ATCC. Viability was determined by trypan blue staining and all counts were done on the Invitrogen Countess cell counting system. Average viability was calculated to be 95% with an average yield of 4–5 $\times 10^6$ cells/mL. Cells were not pre-sorted prior to culture, and were cultured within 2 h of processing. T-cell population was determined by CD4 and CD8 surface staining at time of analysis by flow cytometry. Baseline viability after culture was determined by scatter plots of non-cultured primary lymphocytes.

4.2. Synthetic peptides and proteins

Synthetic peptides PL120131 (Ac-GADYKRITVKVN-NH₂) and PD6478 (Ac-MLNWNRLSPSNQTEK-NH₂) were synthesized by

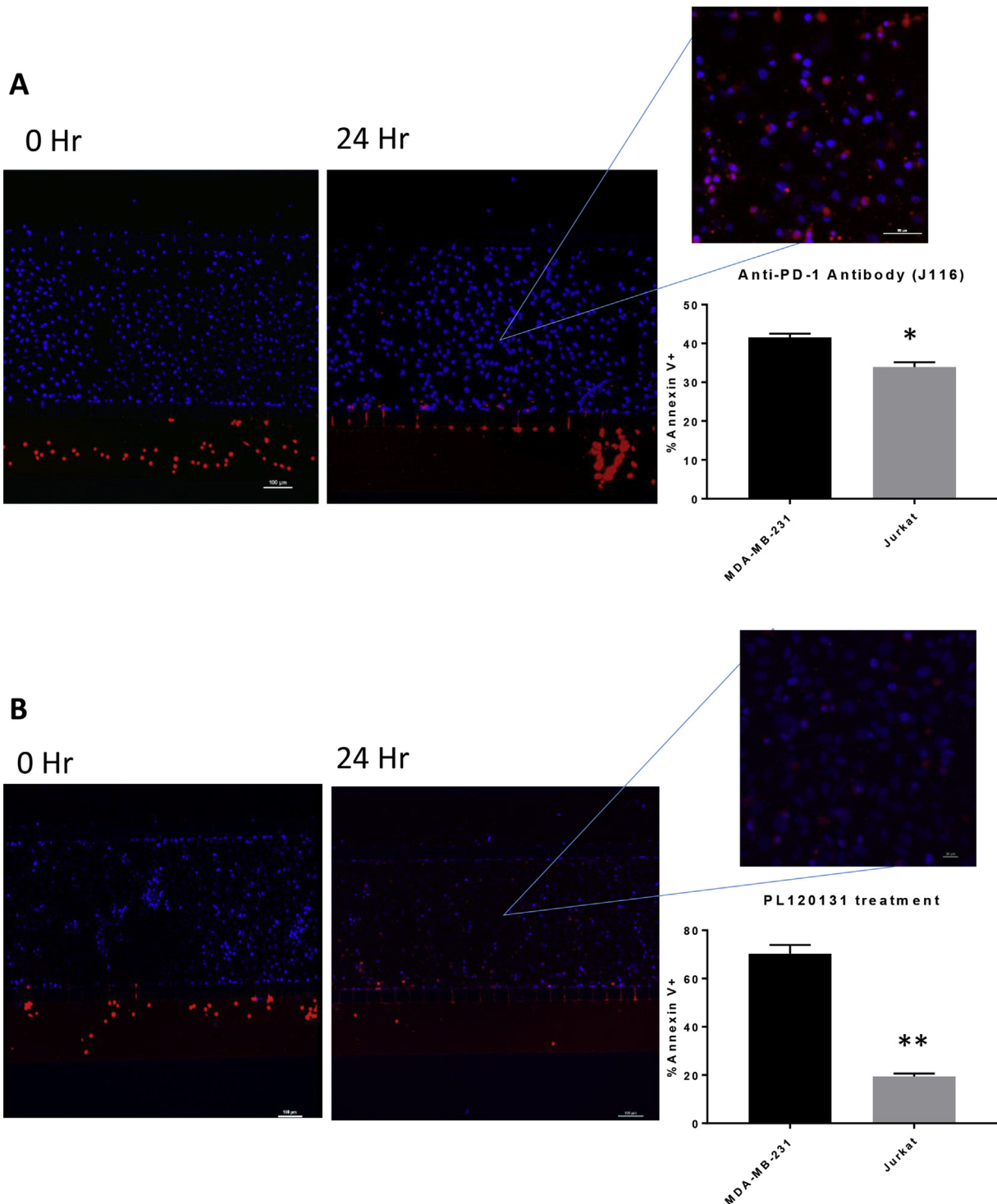


Fig. 7. PL120131 treatment facilitates migration into tumor environments and results in tumor cell death. MDA-MB-231 cells (DAPI stained) were seeded into the central chamber of a micro-fluidics slide, using human fibronectin as the extracellular matrix. Jurkat cells (CellTracker Red) pre-treated with either PD-1 blocking antibody (A) or PL120131 (B) were then passed through the “vascular” chamber of the slide. The slide was imaged by confocal microscope at 0 h and again at 24 h. Cells in the central chamber were trypsinized and collected for expression of Annexin V by flow cytometry. Student’s t-test was used to analyze flow cytometry data for 3D co-culture. $P < 0.05 = *$, $P < 0.005 = **$, $P < 0.0001 = ***$. Each condition was tested in duplicate. Flow cytometry was based on replicate analysis of 5000 events.

Biomatik to >98% purity and were dissolved from lyophilized powder in sterile milli-Q H₂O to a stock concentration of 5 mM for use in all binding and *in vitro* assays. Peptides were synthesized with acetyl and amide groups capping the N- and C- termini, respectively to aid in stability. Similarly, synthetic PD-1 and PD-L1

were purchased from Acro Biosystems and diluted in sterile PBS according to manufacturer’s protocol to stock concentration of 200 µg/mL. All synthetic proteins and peptides were aliquoted to prevent degradation from repeated freeze thaw cycles.

4.3. Luciferase based PD-1/PD-L1 blockade assay

Checkpoint blockade was assayed by the PD-1/PD-L1 blockade luciferase reporter assay (Promega). Briefly, PD-L1 APC/CHO-K1 stably expressing cells were thawed in Ham's F-12 media containing 10%FBS. The cells were plated in a tissue culture treated, white 384 well plate at 5000 cells/10 μ L/well and allowed to incubate overnight. The following day, PD-1 expressing effector cells (Jurkat cells) in RPMI1640 with 1% FBS were plated separately at a concentration of 10,000 cells/20 μ L per well. The effector cells were then treated with a 10-point serial dilution of vehicle, anti-PD-1 blocking antibody, PD6478, or PL120131 for 30 min at 37 °C before being transferred to the plate containing the CHO cells. The co-culture was then incubated at 37 °C for 6 h in a tissue culture incubator. Following incubation, the Bio-Glow reagent was added to the wells in a 1:1 ratio and incubated for 10 min at room temperature. Luminescence was measured from the top down on a Synergy4 (BioTek) plate reader with an integration time of 0.5 s. Data was analyzed by GraphPad Prism 7.

4.4. Computational modeling

Initial docking simulations were conducted using the CABS-Dock server for flexible protein-peptide docking. The theoretical peptide PL120131 was modeled blindly against the extracellular domain of Human PD-1 (PDB 3RRQ). Cluster density, average RMSD and max RMSD were calculated as part of the CABS-Dock process [24,25]. Computational modeling and docking simulations were run on the MOE 2015.10 molecular modeling and simulations software (Chemical Computing Group). The extracellular domain of the human PD-1 protein, PDB ID 3RRQ, was used as the coordinate file. The solved structure of PD-1 was then placed in a virtual environment that neutralized the charges, solvated the structure with waters using the R-Field 1:80 algorithm, and applied the AMBER10:EHT force field. After energy minimization to determine the lowest energy conformation, the 12-mer PD-L1 (PL120131) derived peptide sequence was built in the same environment using the protein builder function within MOE. This sequence was also energy minimized to its lowest energy conformation.

To focus the peptide binding to the known PD-L1 interaction site on PD-1, a "site finder" command was run and the resulting residues within that pocket were specified for docking. The PL120131 was then docked in 30 different conformations, recording the top 5 lowest docking energy. The theoretical binding energy (ΔG) was calculated using the docking software MOE (Chemical Computing Group).

4.5. Binding assays

Binding assays were all conducted using biolayer interferometry (BLI) on an OctetRed (Pall ForteBio) with Protein A labeled dip-and-read biosensors. Either recombinant FC-PD-1 or Fc-PD-L1 was loaded onto the biosensors at a concentration of 8 μ g/mL. Loading was done for 300s, followed by a baseline reading then an association reading for 300s followed by a 600s dissociation reading. Amounts of PL120131 ranged in concentration from 2 μ M to 0.024 μ M in 3:1 serial dilutions for initial binding experiments and 120–1.25 μ M for inhibition studies. Binding data was analyzed using the Octet software analysis system. For inhibition studies, peptide concentration varied while protein concentration was held constant.

4.6. Synthetic peptides and proteins

Synthetic peptides PL120131 (Ac-GADYKRITVKVN-NH₂) and

PD6478 (Ac-MLNWNRLSPSNQTEK-NH₂) were synthesized by Biomatik to >98% purity and were dissolved from lyophilized powder in sterile milli-Q H₂O to a stock concentration of 5 mM for use in all binding and *in vitro* assays. Peptides were synthesized with acetyl and amide groups capping the N- and C- termini, respectively to aid in stability. Similarly, synthetic PD-1 and PD-L1 were purchased from Acro Biosystems and diluted in sterile PBS according to manufacturer's protocol to stock concentration of 200 μ g/mL. All synthetic proteins and peptides were aliquoted to prevent degradation from repeated freeze thaw cycles.

4.7. Luciferase based PD-1/PD-L1 blockade assay

Checkpoint blockade was assayed by the PD-1/PD-L1 blockade luciferase reporter assay (Promega). Briefly, PD-L1 APC/CHO-K1 stably expressing cells were thawed in Ham's F-12 media containing 10%FBS. The cells were plated in a tissue culture treated, white 384 well plate at 5000 cells/10 μ L/well and allowed to incubate overnight. The following day, PD-1 expressing effector cells (Jurkat cells) in RPMI1640 with 1% FBS were plated separately at a concentration of 10,000 cells/20 μ L per well. The effector cells were then treated with a 10-point serial dilution of vehicle, anti-PD-1 blocking antibody, PD6478, or PL120131 for 30 min at 37 °C before being transferred to the plate containing the CHO cells. The co-culture was then incubated at 37 °C for 6 h in a tissue culture incubator. Following incubation, the Bio-Glow reagent was added to the wells in a 1:1 ratio and incubated for 10 min at room temperature. Luminescence was measured from the top down on a Synergy4 (BioTek) plate reader with an integration time of 0.5 s. Data was analyzed by GraphPad Prism 7.

4.8. Flow cytometry

All flow cytometry experiments were acquired on the Intellicyt iQue⁺ screener (Intellicyt). Cell Surface markers CD3 and CD8, as well as the chemokine marker Granzyme B for immune profiling, were all from BioLegend. The Multicyt Apoptosis kit (Intellicyt) was used for evaluation of apoptotic activity by Annexin V and Caspase 3/7 activity. Cell culture was treated for 6 h prior to staining with GolgiStop supplied in the BD Cytofix/Cytorperm Plus kit. The data acquired by the Intellicyt was analyzed by the Forecyt analysis software.

4.9. Cytokine analysis

4T1 cells were at 20,000 cells/well in 96-well flat bottom plate and allowed to culture overnight. The following day, mouse lymphocytes, isolated from lymph nodes and homogenized through 40 micron mesh, were plated in co-culture at a count of 40,000 cells/well in a total of 100 μ L. Ten-point 2X dosing was done at top concentration of 25 μ g/mL. Three dosing points (high, median, and low) were selected and added to the plate with J116 anti-PD-1 as a positive control.

After 24 h culture, the plates were spun down and the supernatant collected. According to the protocol provided in the Multicyt Q Beads PlexScreen Secreted Protein Assay Kit (Intellicyt), 10 μ L of supernatant was incubated with a 10 μ L cocktail of 1x capture beads (IL-10, IL-12p70, CCL4, and IFN γ) for 1 h. Then, 10 μ L of detection reagent was added for a final volume of 30 μ L in a v-bottom 384-well assay plate. The samples were read on the iQue Screener Plus (Intellicyt). Concentration were determined based on a standard curve for each protein.

4.10. Jurkat migration into tumor microenvironment

The central chamber of a SynVivo microfluidics chip (Supplemental Fig. 1) was coated with human fibronectin (Calbiochem 341635) at a concentration of 200 µg/mL under 6 p.s.i. constant pressure to ensure that no air bubbles were introduced. The external chambers were filled with sterile PBS and the chip was incubated overnight at 4 °C. 5.0×10^6 MDA-MB-231 cells in L-cell conditioned DMEM were then seeded into the central chamber at a constant flow rate of 5 µL/min. The cells were allowed to attach in the fibronectin overnight at 37 °C.

CellTracker Red CMTPX (Invitrogen) was added to 2×10^6 Jurkat cells at a concentration of 2 µM (in the dark) and placed in the incubator overnight. The following day, the MDA-MB-231 cells were washed with fresh conditioned L-cell media to remove any non-adherent cells. The cells were then stained with Hoechst stain in L-cell media for 15 min.

Stained Jurkat cells were treated with either Anti-PD-1 (clone J116) or PL12031 at a concentration of 30 µM for 30 min. The Jurkat cells were then injected into the outer chamber at a physiological flow rate of 0.2 µL/min for 24 h. Confocal live-cell imaging was used to ensure that cells were adequately stained and Jurkat cells were flowing in the outer chamber. After 24 h, cells from the central chamber were trypsinized, collected, and stained for Annexin V. The cells were assessed for cell death by flow cytometry.

4.11. Statistics

Data analysis was done by calculating measures of central tendency (sample mean, sample median) and dispersion (sample variance, interquartile range for different phenotypic markers). Histograms and scatterplots were developed to visually inspect the distribution of the outcome (histogram) and the relationship between outcomes (expression levels) and dose level of peptide (scatterplot). Measurements were collected at 7 dose levels with 3 measurements collected at each dose level. With 21 observations, an ordinary least square regression was utilized to fit a polynomial dose response curve. 21 observations provided 95% power to detect a smaller R2 of 51% using a Type I error rate of 0.05. R² value of 0.8 is considered a significant response. For flow cytometry analysis, 2 way ANOVA was used for dose response experiments and Student's t-test was used for single dose measurements.

Author contributions

Experiments were conceived and designed by R. B., M.S. and B.X. Experiments and data analysis were performed by R.B., I.S., J.M., and V.S. Overall discussions of the data and implications involved all authors; and the manuscript was written by R.B. and B.X.

Competing financial interests

None.

Acknowledgements

This work was supported by funds from the Alabama Cancer Research Consortium, the Alabama Innovation Fund, New Investigator Award from the University of Alabama at Birmingham Comprehensive Cancer Center Young Supporter's Board, 2016YFC0904601 from the Ministry of Science and Technology, and the National Natural Science Foundation of China (81672743).

Appendix A. Supplementary data

Supplementary data related to this article can be found at <https://doi.org/10.1016/j.canlet.2018.04.031>.

References

- [1] A.H. Sharpe, G.J. Freeman, The B7-CD28 superfamily, *Nat. Rev. Immunol.* 2 (2002) 116–126.
- [2] H. Chang, W.Y. Jung, Y. Kang, H. Lee, A. Kim, H.K. Kim, et al., Programmed death-ligand 1 expression in gastric adenocarcinoma is a poor prognostic factor in a high CD8+ tumor infiltrating lymphocytes group, *Oncotarget* 7 (2016) 80426–80434.
- [3] Y. Ishida, Y. Agata, K. Shibahara, T. Honjo, Induced expression of PD-1, a novel member of the immunoglobulin gene superfamily, upon programmed cell death, *EMBO J.* 11 (1992) 3887–3895.
- [4] M.E. Keir, M.J. Butte, G.J. Freeman, A.H. Sharpe, PD-1 and its ligands in tolerance and immunity, *Annu. Rev. Immunol.* 26 (2008) 677–704.
- [5] D.F. McDermott, M.B. Atkins, PD-1 as a potential target in cancer therapy, *Cancer Med.* 2 (2013) 662–673.
- [6] Q. Wang, F. Liu, L. Liu, Prognostic significance of PD-L1 in solid tumor: an updated meta-analysis, *Medicine* 96 (2017), e6369.
- [7] P. Wu, D. Wu, L. Li, Y. Chai, J. Huang, PD-L1 and survival in solid tumors: a meta-analysis, *PLoS One* 10 (2015), e0131403.
- [8] D.F. McDermott, M.M. Regan, M.B. Atkins, Interleukin-2 therapy of metastatic renal cell carcinoma: update of phase III trials, *Clin. Genitourin. Canc.* 5 (2006) 114–119.
- [9] T. Zenz, Exhausting T cells in CLL, *Blood* 121 (2013) 1485–1486.
- [10] S.A. Fuertes Marraco, N.J. Neubert, G. Verdeil, D.E. Speiser, Inhibitory receptors beyond T cell exhaustion, *Front. Immunol.* 6 (2015) 310.
- [11] Y. Jiang, Y. Li, B. Zhu, T-cell exhaustion in the tumor microenvironment, *Cell Death Dis.* 6 (2015), e1792.
- [12] L. Pai-Scherf, G.M. Blumenthal, H. Li, S. Subramaniam, P.S. Mishra-Kalyani, K. He, et al., FDA approval summary: pembrolizumab for treatment of metastatic non-small cell lung cancer: first-line therapy and beyond, *Oncologist* 22 (11) (2017 Nov) 1392–1399.
- [13] D. Kazandjian, D.L. Suzman, G. Blumenthal, S. Mushti, K. He, M. Libeg, et al., FDA approval summary: Nivolumab for the treatment of metastatic non-small cell lung cancer with progression on or after platinum-based chemotherapy, *Oncology* 21 (2016) 634–642.
- [14] N. Seetharamu, I.R. Preeshagul, K.M. Sullivan, New PD-L1 inhibitors in non-small cell lung cancer - impact of atezolizumab, *Lung Canc.* 8 (2017) 67–78.
- [15] H. Linardou, H. Gogas, Toxicity management of immunotherapy for patients with metastatic melanoma, *Ann. Transl. Med.* 4 (2016) 272.
- [16] D.Y. Lin, Y. Tanaka, M. Iwasaki, A.G. Gittis, H.P. Su, B. Mikami, et al., The PD-1/PD-L1 complex resembles the antigen-binding Fv domains of antibodies and T cell receptors, *Proc. Natl. Acad. Sci. U. S. A.* 105 (2008) 3011–3016.
- [17] K. Guzik, K.M. Zak, P. Grudnik, K. Magiera, B. Musielak, R. Torner, et al., Small-molecule inhibitors of the programmed cell death-1/programmed death-ligand 1 (PD-1/PD-L1) interaction via transiently induced protein states and dimerization of PD-L1, *J. Med. Chem.* 60 (2017) 5857–5867.
- [18] Q. Li, L. Quan, J. Lyu, Z. He, X. Wang, J. Meng, et al., Discovery of peptide inhibitors targeting human programmed death 1 (PD-1) receptor, *Oncotarget* 7 (2016) 64967–64976.
- [19] G.P. Mogno, R. Spreafico, V. Wong, J.P. Scott-Browne, S. Togher, A. Hoffmann, et al., Exhaustion-associated regulatory regions in CD8(+) tumor-infiltrating T cells, *Proc. Natl. Acad. Sci. U. S. A.* 114 (2017) E2776–E2785.
- [20] J.M. Rosano, N. Tousi, R.C. Scott, B. Krynska, V. Rizzo, B. Prabhakarandian, et al., A physiologically realistic in vitro model of microvascular networks, *Bio-med. Microdevices* 11 (2009) 1051–1057.
- [21] B. Prabhakarandian, M.C. Shen, J.B. Nichols, C.J. Garson, I.R. Mills, M.M. Matar, et al., Synthetic tumor networks for screening drug delivery systems, *J. Contr. Release: Official. Contr. Release Soc.* 201 (2015) 49–55.
- [22] T.B. Terrell-Hall, A.G. Ammer, J.I. Griffith, P.R. Lockman, Permeability across a novel microfluidic blood-tumor barrier model, *Fluids Barriers CNS* 14 (2017) 3.
- [23] T.A. Aguilera, A.J. Giaccia, Molecular pathways: oncologic pathways and their role in t-cell exclusion and immune evasion—a New role for the AXL receptor tyrosine kinase, *Clin. Canc. Res. Official J. Am. Assoc. Cancer Res.* 23 (2017) 2928–2933.
- [24] M. Kurcinski, M. Jamroz, M. Blaszczyk, A. Kolinski, S. Kmiecik, CABS-dock web server for the flexible docking of peptides to proteins without prior knowledge of the binding site, *Nucleic Acids Res.* 43 (2015) W419–W424.
- [25] M. Blaszczyk, M. Kurcinski, M. Kouza, L. Wieteska, A. Debinski, A. Kolinski, et al., Modeling of protein-peptide interactions using the CABS-dock web server for binding site search and flexible docking, *Methods* 93 (2016) 72–83.